Analysis on Averaging Lorenz System and its application to climate

A THESIS

SUBMITTED TO THE FACULTY OF THE GRADUATE SCHOOL

OF THE UNIVERSITY OF MINNESOTA

BY

Yiran Shi

IN PARTIAL FULFILLMENT OF THE REQUIREMENTS

FOR THE DEGREE OF

MASTER OF SCIENCE

Richard McGehee

August, 2021

Acknowledgements

First, I would like to express my most sincere appreciation to my advisor, Richard McGehee, for his continuous support and guidance of my thesis. Without him, I cannot imagine how to make this work possible. Under his guidance of my master study, I am grateful to have the opportunity to explore the area of climate and math.

I would also like to thank all other professors, Arnd Scheel, Christine Berkesch, Maria-Carme Calderer, Paul Garrett, Richard Moeckel and Victor Reiner, who have taught me or inspired me during my graduate studies. I have benefited in many ways from their excellent teaching.

Lastly I would like to thank my parents, Jianwei Shi and Aiwu Liu, for spiritually and financially supporting me throughout my life. Especially during this COVID-19 pandemic, their encouragement allows me to pursue my dream without concerns.

Dedication

This thesis is dedicated to my parents, Mr. Shi and Mrs. Liu who greatly support me through this pandemic, and to my friends who spiritually encourage me.

Abstract

The chaotic nature of weather systems was firstly discovered by Edward Lorenz, who was a mathematician and meteorologist and well-known for the discovery of "Butterfly effect". Since then, Chaos Theory triggered many interests in physics and ecology, as well as climate science. According to him, the natural system lacks periodicity, and weather cannot be predicted for a long time (Lorenz, 1963). A small inaccuracy could lead to a prediction that is the opposite of what happens in the future. For example, we cannot exactly predict the weather in Minneapolis at 10am on the 15th June 2022, whereas we can predict the average temperature of the summer based on previous data. The behavior of basic Lorenz System is highly-studied by many mathematicians and well-understood. Nevertheless, the study of averaging Lorenz system has not gone into very thoroughly.

This thesis analyzes the behavior of averaging Lorenz system and its feasibility to climate phenomenons. To achieve the goal, I first examine the nature of averaging Lorenz system using several different time steps. The different typical behaviors of averaged Lorenz model are thoroughly studied. Then, I analyze the dynamics of averaged Lorenz system from multiple different perspective and show the main conclusion that the averaged system induces higher predictability. Finally, I simulate the model for recent 50-years' El Nino and compare it with the averaging system I got.

Contents

List of Figures

Chapter 1

Introduction

Before doing anything formal, let us first interpret the term "chaos". From day-to-day life, it means a state which is in complete confusion. Mathematically, we need a more exact definition. One of the most essential features of "chaos" is the sensitive dependence on initial conditions, which leads to the story of how Lorenz found chaos. Back in the 1960s, Lorenz was studying weather at MIT. He simulated a weather model without being able to predict the results. One day he decided to repeat those simulations as he mentioned in his book 'The Essence of Chaos':

"At one point, I decided to repeat some of the calculations in order to examine what was happening in greater detail. I stopped the computer, typed in a line of numbers that had come out of the printer a little earlier, and started it back up. I went to the lobby to have a cup of coffee and came back an hour later, during which the computer had simulated about two months of weather. The numbers coming out of the printer had nothing to do with the previous ones."

The truth is that he did not type in the exact numbers as the previous ones. He rounded those numbers and assumed those tiny enough errors would be insignificant. However,

those tiny errors began to grow exponentially as model ran, and the outcome was completely different from the earlier ones. This phenomenon was later defined as "chaos". For weather models, every single state has to be known in order to make an accurate prediction, which is impossible by Heisenberg uncertainty principle. Hence, it is impossible to predict future weather in a long term (Lorenz, 1963). But if the movement of every molecule in the weather is know, Lorenz also mentioned that the short term prediction is possible.

Even though long-term weather is hard to predict, it may be possible to predict the climate since we are not trying to predict the exact weather conditions, but their average over a certain period. It is shown by some people, such as Dwivedi and Mittal (2007), that the averaged prediction is workable and actually has higher predictablity which means the error does not matter significantly. For example, if we are trying to forecast the next El Nino event, we can simulate the development of sea surface temperature on central pacific. Run the model for a long enough time and take the sliding average over a certain period, if the overall trend is in the direction of warming, then it is likely to have a strengthening El Nino.

The ultimate Lorenz equations, after Lorenz's years of work, are three nonlinear differential equations in terms of three variables. Despite its simplicity, this model behaves in a chaotic and unpredictable way, which is highly sensitive to initial conditions. Its chaotic behavior is not only caused by the error, but is also an intrinsic property of the model. In general, there does not exist an widely accepted definition of the term "chaos". But I will use an easy-to-understand definition from S.H. Strogatz (1994):

"Chaos is aperiodic long-term behavior in a deterministic system that exhibits sensitive dependence on initial conditions."

To begin, let us think about how the averaged climate behaves. Global temperature is a nice example to illustrate the long-time average behavior of weather. Figure 1.1 is the change in global temperature in recent years. The data comes from NOAA National Centers for Environmental information and they use the 20th century average of global temperature as a zero line. Figure 1.2 is the 30-year average of global temperature. Both figures demonstrate that the global temperature is gradually increasing without any periodic pattern. So to some extent, taking a long-term average is feasible for some events, at least for global temperature which is not a periodic event.

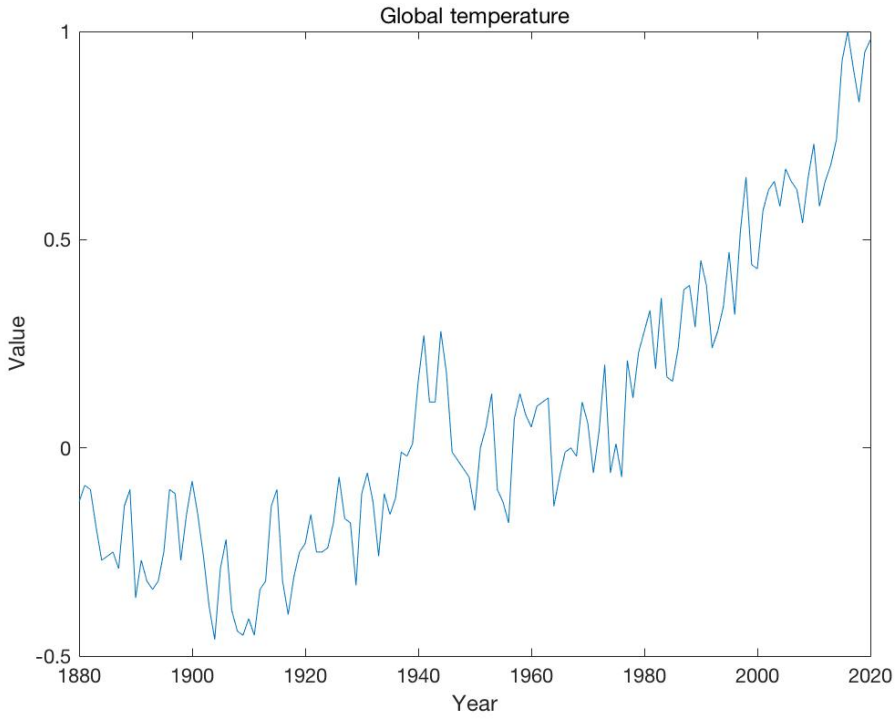

Figure 1.1: Change in Global Temperature from 1880 to 2020 (data collected from NOAA National Centers for Environmental information)

For other periodic climate events, such as El Nino and Southern Oscillation (ENSO) which happens around 6-8 years, taking a long-term average does not give a dominant trend. The average sea surface temperature is one of the main signs forecasting the

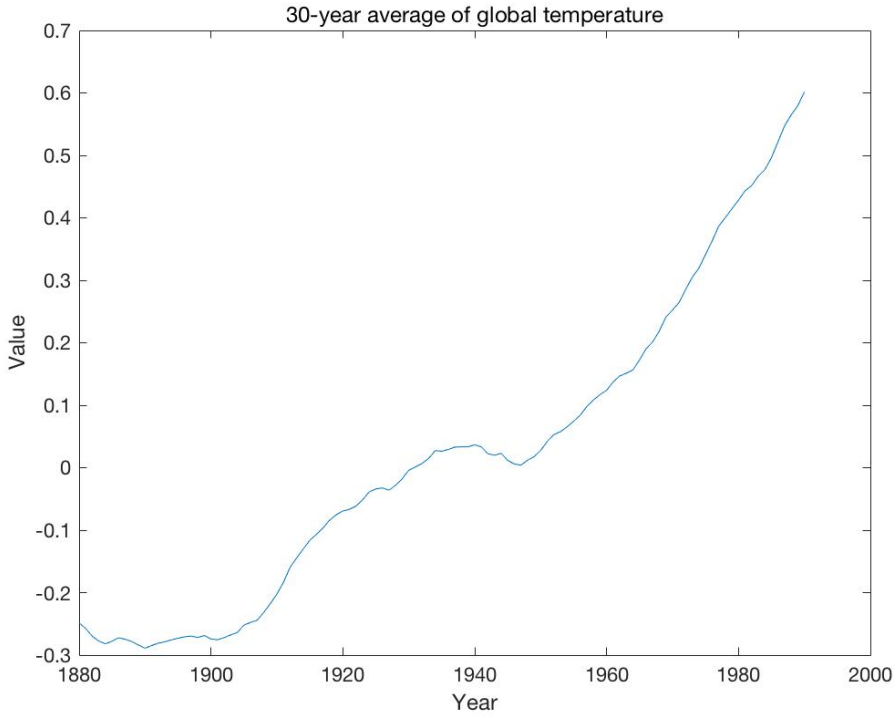

Figure 1.2: 30-year average of Global Temperature from 1880 to 2020

occurrence of ENSO and is supposed to have a precise frequency. Figure 1.3 is the oceanic Nino index for ENSO which alternates between 2.5 and -2, indicating the occurrence of El Nino and La Nina respectively. However, its long-term average, which is shown in Fig 1.4, does not represent the actual occurrence of events. The averaging ONI oscillates between 0.15 and -0.15, which is defined as the regular session and no events happen. This illustrates that taking a long-term average does not always work for climate events. However, as described below in Chapter 4, the cusp map provides some information, and it explains the nature of climate events very well.

I will mainly examine the behaviors and properties of the averaged Lorenz system over several different periods in this work, and analyze its practicability. Chapter 2 gives

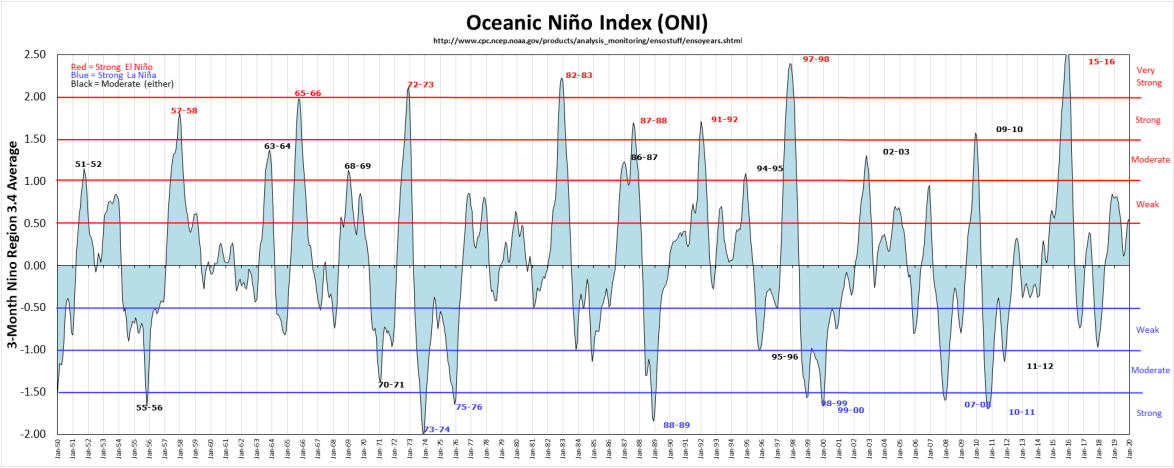

Figure 1.3: ONI of ENSO from 1950 to 2019 (data collected from National Weather Service, graphed by Golden Gate Weather Services)

some background of Lorenz system, including its chaotic behavior. Chapter 3 presents the phase space of Lorenz system averaged over different time period and analyses from multiple perspectives. Chapter 4 analyzes the behavior of cusp map. Chapter 5 concludes the observation and gives some results. Chapter 6 discusses the feasibility of averaged system to ENSO and chapter 7 presents possible future work.

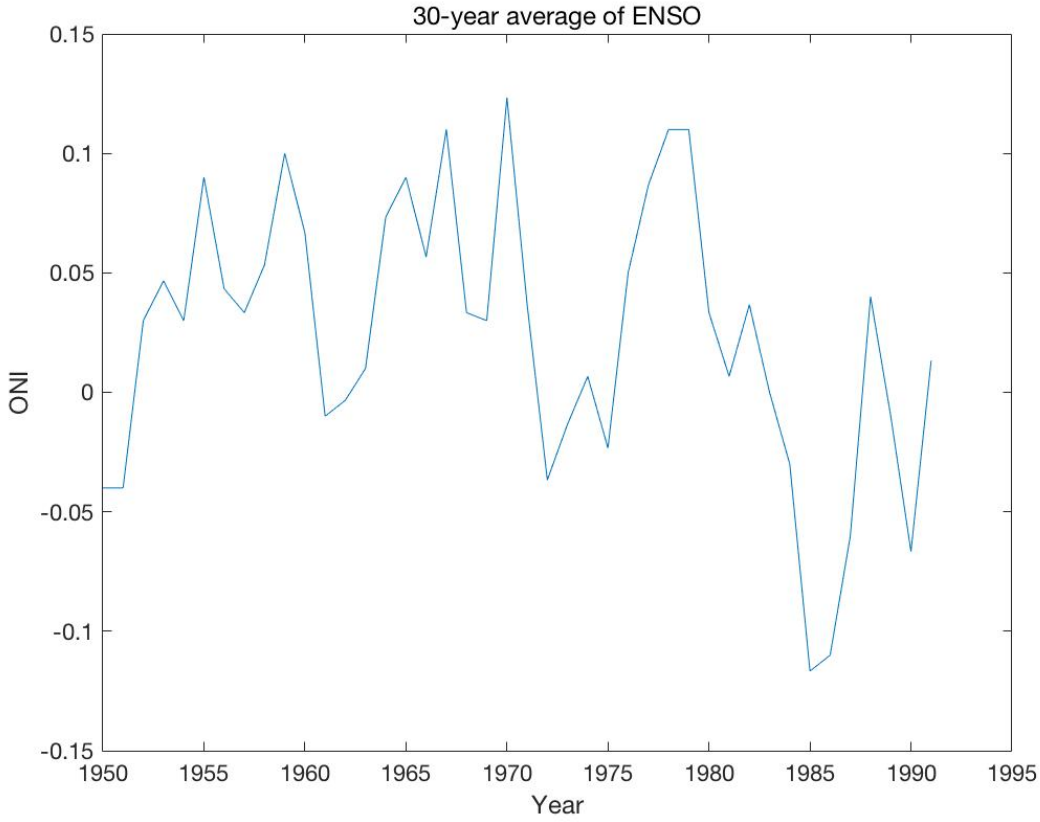

Figure 1.4: 30-year average of ONI of ENSO from 1950 to 2019 (data collected from National Weather Service, graphed by Golden Gate Weather Services)

Chapter 2

Background

2.1 Dynamics of Lorenz System

2.1.1 Equilibriums of Lorenz Equations

The Lorenz System is given by

$$\dot{x} = \sigma(y - x)$$
$$\dot{y} = rx - y - xz$$
$$\dot{z} = xy - bz$$

where parameters $\sigma, r, b > 0$. These parameters do have physical meaning, and can be considered as the Prandl number, the Rayleigh number, and the wave length number, respectively. Typical parameter value $\sigma = 10, r = 28, b = \frac{8}{3}$ gives an chaotic system which are commonly used to model the Earth's atmosphere, and all discussion in this work uses these values (Black et al., 2010). In general, there are always three equilibriums: $(0, 0, 0)$, $(-\sqrt{b(r-1)}, -\sqrt{b(r-1)}, r-1)$, and $(\sqrt{b(r-1)}, \sqrt{b(r-1)}, r-1)$ by setting $\dot{x} = \dot{y} = \dot{z} = 0$. One of the basic properties of these equations is that they are invariant under transformation $(x, y, z) \to (-x, -y, z)$, which can be seen from the location of equilibrium points. On figure 2.1, the two equilibrium points are the centers of two

manifolds. To study the dynamics of the system, it is important to firstly study the stability of these equilibrium points. The model constructed by using $\sigma = 10, r = 28, b = \frac{8}{3}$ is shown in figure 2.1.

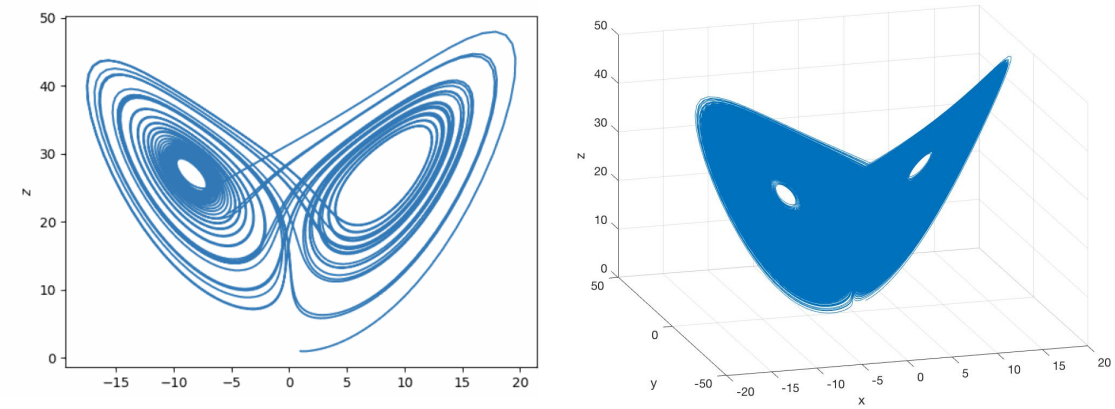

(a) 2D plot using axis x-z

(b) 3D plot

Figure 2.1: 2D and 3D plots of Lorenz Equations using parameters $\sigma = 10, r = 28, b = \frac{8}{3}$

2.1.2 Stability

To analyze the stability of the equilibriums, let us only consider the case when $r > 1$ since this is what I will mainly focus on throughout this thesis. The Jacobi matrix of Lorenz System by using $\sigma = 10, r = 28, b = \frac{8}{3}$ is

$$J = \begin{bmatrix} -\sigma & \sigma & 0 \\ r - z & -1 & -x \\ y & x & -b \end{bmatrix} = \begin{bmatrix} -10 & 10 & 0 \\ 28 - z & -1 & -x \\ y & x & -\frac{8}{3} \end{bmatrix}$$

At $(x, y, z) = (0, 0, 0)$, the corresponding matrix J has one positive eigenvalue, 11.8277, which implies that the origin point is unstable. All points start close to origin will eventually leave this region. For the other two equilibriums $(-\sqrt{b(r-1)}, -\sqrt{b(r-1)}, r-1)$,

and $(\sqrt{b(r-1)}, \sqrt{b(r-1)}, r-1)$, their corresponding Jacobi matrix has a negative eigenvalue and two imaginary eigenvalues with positive real parts. Hence, the other two equilibriums are unstable. So the Lorenz attractor is not a stable equilibrium. In fact, almost all trajetories will approach the lorenz attractors but never reach the equilibrium. The trajectories for the other two equilibriums can be seen from figure 2.1. If we use a slightly different set of parameters, the general form of the system won't change even though the details will be different.

2.1.3 Sensitive to initial condition

The main property of Lorenz System is their sensitive dependence on initial values. Let us consider two initial conditions which differ by a small value: (2,5,1) and (2,5,1.01). Their orbits are shown in Figure 2.2 below. The red orbit is the plot for (2,5,1) and the blue one is for (2,5,1.01). Since the figure is only plotted for the first 1500 iterations, the two orbits differ at least after 1500 iterations. Similarly, I also plot the comparison of these two orbits in each variable which is shown in figure 2.3. All these graphs are plotted using fourth-order Runge-Kutta method with the time step $h = 0.01$. It is shown from the graph that for the first 1500 iterations, the two orbits are identical. However, they seem to differ after at least 1500 iterations. This property makes the long term prediction impossible.

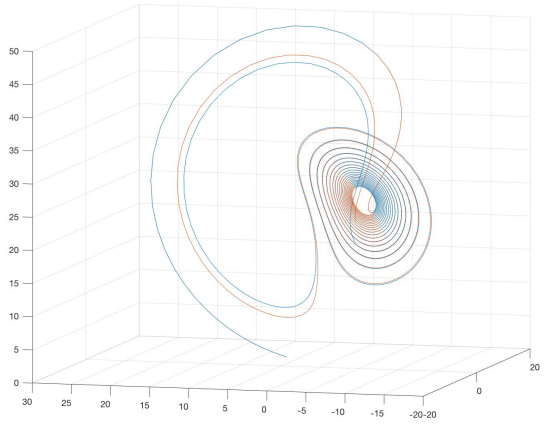

Figure 2.2: comparison between orbits of initial values (2,5,1) and (2,5,1.01).

The graphs illustrate that two points start close to each other will eventually separate apart. A useful tool to analyze this difference is Lyapunov Exponent. It measures how a system varies with small change in initial condition and is often used in studying dynamical system (Wolf et al., 1985). Briefly, consider two trajectories $x(t) = f^t(x_0)$ and $x(t) + \delta x(t) = f^t(x_0 + \delta x(0))$ that start very close to each other, or $\delta \to 0$, their difference is given by $|\delta x(t)| \sim e^{\lambda t}|\delta x(0)|$, where λ, the average rate of separation, is the Lyapunov exponent. The equation proves that two trajectories will separate exponentially with time. Hence, long term prediction is impossible since a small error may lead to two completely different models and error is inevitable for a long time run.

2.2 Chaotic Attractor

The attractors describes the long term behaviors of the system since any trajectory will approach the attractor after some time (Barnett, 1996). And one can understand dynamics of a system just by analyzing its attractors. Lorenz attractors are refered as "strange attractor" because its relevant dynamics is chaotic: it's neither stable/unstable nor periodic. Two symmetric equilibriums of the Lorenz System are the centers for the

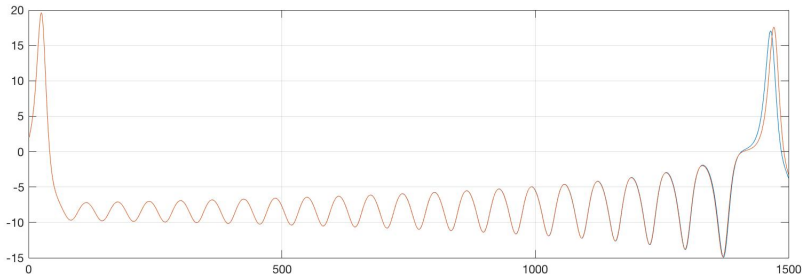

comparison between two orbits in x

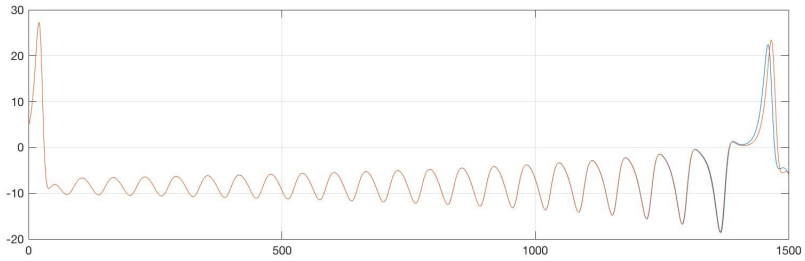

comparison between two orbits in y

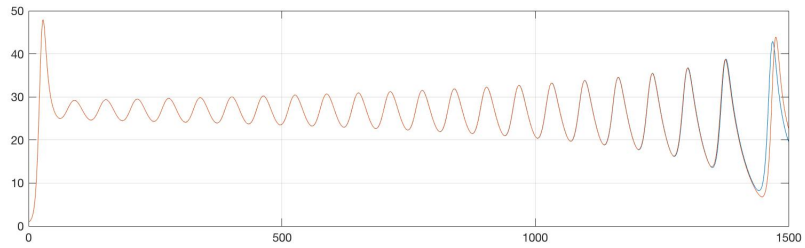

comparison between two orbits in z

Figure 2.3: comparison between orbits of initial values in each variable.

Lorenz Attractors since other trajectories will wander around these two points. However, Lorenz map does not have the shape of a circle or a torus, but rather in a shape of "butterfly" in three-dimension. Tractories of lorenz system are aperiodic. Fig 2.4 is a nice picture of the model drawn by Abraham and Shaw.

The trajectory will firstly stick on one part of the figure, then transfer to the other part, and then back again. All orbits wander around two chaotic attractors, neither cross each other nor repeat.

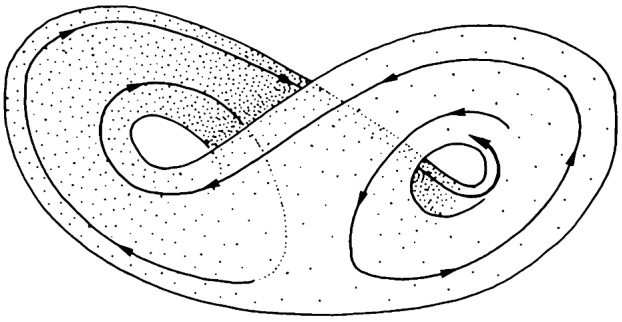

Figure 2.4:]
Lorenz Attractor (Abraham Shaw Dynamics–The Geometry of Behavior,Part Two: Chaotic Behavior[7] p.88

With the basic understanding of the dynamics of Lorenz System, let us discuss the main work of this thesis: the averaging Lorenz system.

Chapter 3

Analysis on Averaging Lorenz System and Its Predictability

3.1 Averaged Lorenz System using different time step

For the discussion in this chapter, I will always use the typical parameter value $\sigma = 10, r = 28, b = \frac{8}{3}$ and initial condition $(1, 1.27, 14.132)$. This initial condition is chosen only because it is close to one of the equilibrium. Nevertheless, this choice should not affect the overall results since what we are calculating is the averaging trajectory. The original Lorenz System runs for 20,000 iterations which are 2000 time units by using time step 0.1 and the method of fourth order Runge-Kutta. Instead of using simple average method, I take the sliding average of the system. Using time step 50 as an example, the first point on the averaged Lorenz trajectory is the average of first 50 data of original Lorenz orbit, starting from first point to the 50th point. Then the second point on the averaged orbit is the average of second point with the following 50 points on original orbit and so on. The advantage of using sliding average is that it prevents a great loss of data. In the above example in chapter 2, the averaged system using sliding average should contain only 50 iterations less than the original system.

Because the last 50 points in the trajectory don't have enough following up data to be averaged. But the usual average method which takes each 50 data will drastically reduce the number of data from 20,000 to 400. The sliding average method remains the advantage of time averaging while keep the length of data-set almost the same (Dwivedi et al, 2007). Furthermore, the sliding average helps the averaged model to flow smoothly since the nearby averaged points won't differ a lot. Let us define the sliding time averaged trajectory as follows:

$$a_i = \frac{1}{T}\sum_{n=0}^{T-1} x_{i+n}$$

Here x_i denotes the original trajectory. i ranges over almost all numbers of iterations. a_i is the averaged point at ith state on the averaged trajectory. T is the desired sliding average interval. If $T = 50$, then the sliding average is taking every 50 iterations to average.

The averaging system behaves differently with different time steps, and are entirely different from the original Lorenz system shown in fig 2.1. Moreover, this is illustrated in figure 3.1 which includes four different images with time step T increasing from 50 to 500. In figure 3.1(a) with averaging time step 50, the system no longer remains the shape of a butterfly. Most points are divided into two parts and converge to two symmetric small regions around z=28. In figure 3.1(b) with time step 100, those two converging regions become more apparent, but shrinks to around z=26. Moreover, some points begin to wander around axis x=y=0. With time step 200, the two regions are still there, but this time it has more small loops in the region z=22 to z=26. And more points begin to circle around the middle region. With time step 500, more loops appear and fewer points circle around the two top regions. Notice that these averaged systems are symmetric about axis x=y=0.

Since the size of attracting regions keep shrinking, we expect a higher predictability in the averaged system. The prediction error will become saturated near attractors and the smaller the size of attractors, the higher the predictability will be (Dwivedi et al, 2006).

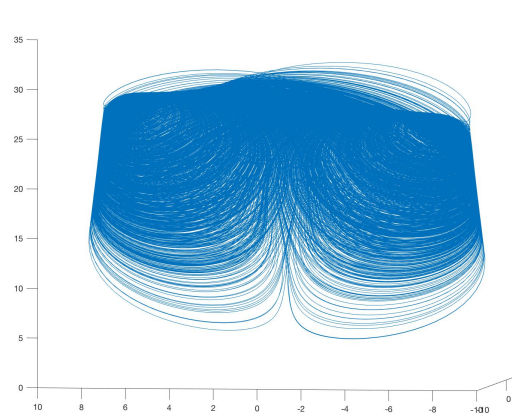

(a) averaged Lorenz model using time step t=50

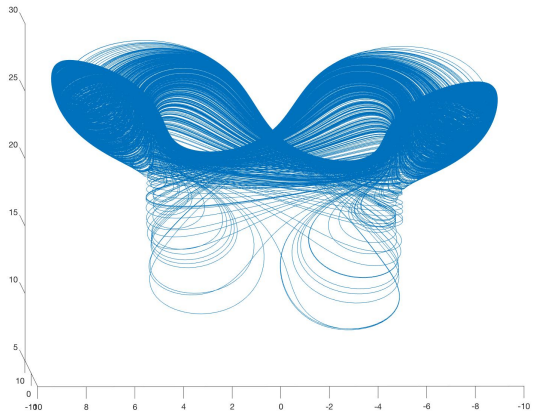

(b) averaged Lorenz model using time step t=100

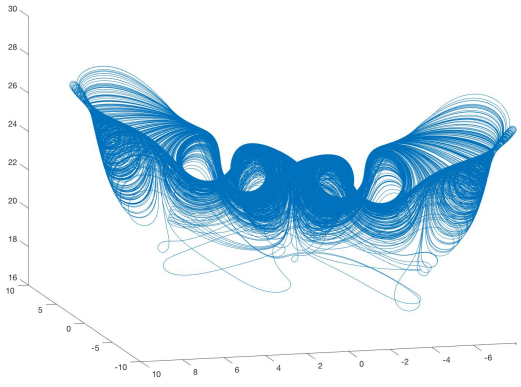

(c) averaged Lorenz model using time step t=200

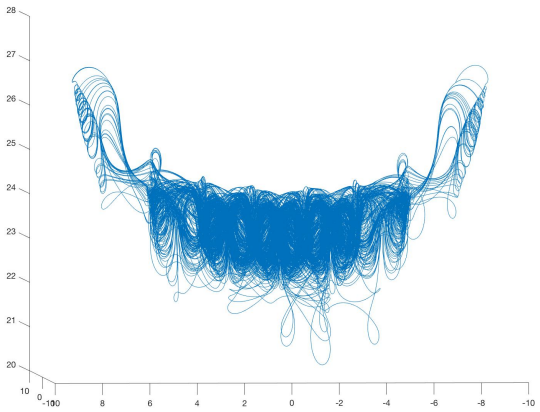

(d) averaged Lorenz model using time step t=500

Figure 3.1: trajectories of the averaged Lorenz system using different time step

3.2 Histogram Analysis of each solution

In order to better understand these figures, let us analyze the histogram in each x,y,z solution which shows the number of points that lies in each region of the solution. This is demonstrated in figure 3.2 and figure 3.3 below. Since the trajectories are symmetric, the histogram on x and y solutions are the same, so only analysis of one of them is presented here. This technique helps to reduce the analysis of the three-dimensional system to one dimension.

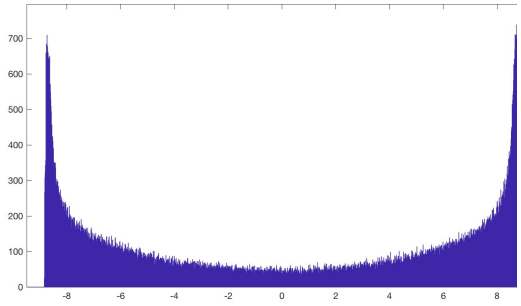

(a) using averaged time step T=50

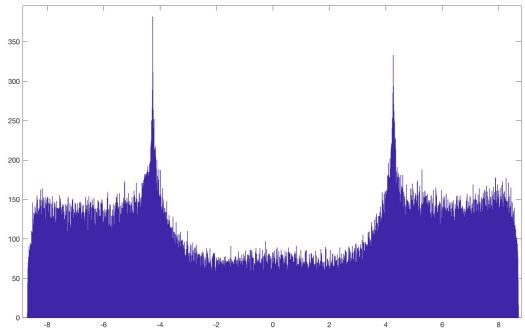

(b) using averaged time step T=100

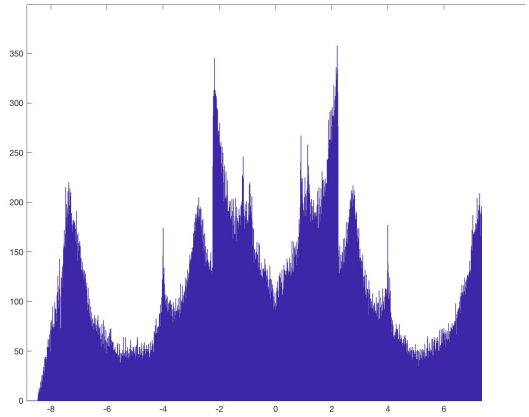

(c) using averaged time step T=200

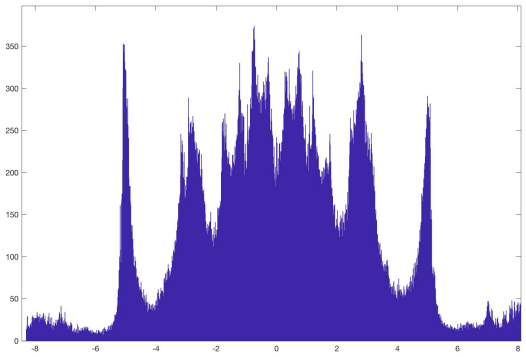

(b)using averaged time step T=500

Figure 3.2: histogram analysis of x solution in averaged Lorenz system which shows the portion of points that lies in different regions

Figure 3.2 shows that those averaged system are indeed symmetric about axis x=y=0 because all figures are symmetric about origin. For $T = 50$, most points lie in the region $x = -8$ and $x = 8$ and only a few points lie in the middle zone $(-7, 7)$. For $T = 100$, less points lie in the region $x = -8$ and $x = 8$ and points start to distribute over the middle zone. However, there are still a small portion of the data lie in the middle section from $x = -2$ to $x = 2$. Using $T = 200$, there are more focus areas. Most points are distributed around $x = -7, -2, 2, 8$. With a larger time step $T = 500$, there are much more concentration areas and we can make the observation that with increasing time step, the number of converging area increases which corresponds to the previous observation that more small loops appear with increasing time step.

From histogram of z-solution, the converging region gradually shrinks. With time step 50, most points converge at around z=28. With time step 100, most points gather around the region from z=20 to z=28. Later, this region shrinks to the region from z=21 to z=25 and eventually shrinks to the region from z=22.5 to z=24.5. Compare to figure 3.3(d), z=22.5 to z=24.5 is the region where loops appear.

3.3 Spectra Analysis

Many natural events are periodic such as El Nino. If the averaging Lorenz system is capable of modeling the pattern of these events, then it ought to be periodic as well. Hence, we want to know if there is an obvious frequency in the averaged system. To achieve the goal, I use the Fast Fourier Transform (FFT). The FFT computes the Discrete Fourier Transform (DFT) in a more efficient algorithm because "it eliminates redundancies that result from adding certain data sequence values after they have been multiplied by the same factors of fixed complex constants during the evaluation of different DFT transform coefficients." (Douglas,1987). FFT allows us to observe the

change in amplitude and identify important frequencies in the data, leading to a more complete picture of dynamics of the nonlinear system (Dietrich,2008). FFT algorithms compute the frequency of a given discrete signal x[n], and the general formulas are listed below.

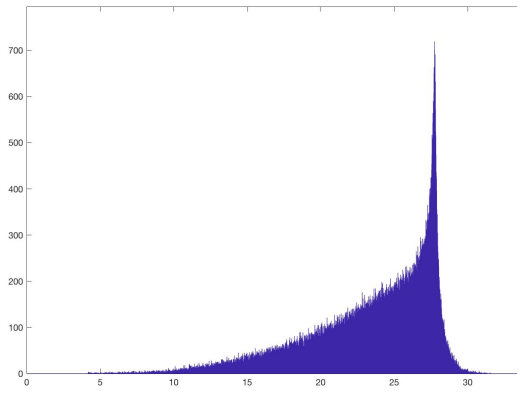

(a) using averaged time step T=50

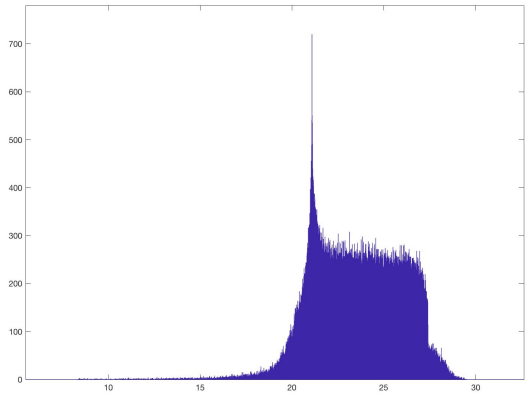

(b) using averaged time step T=100

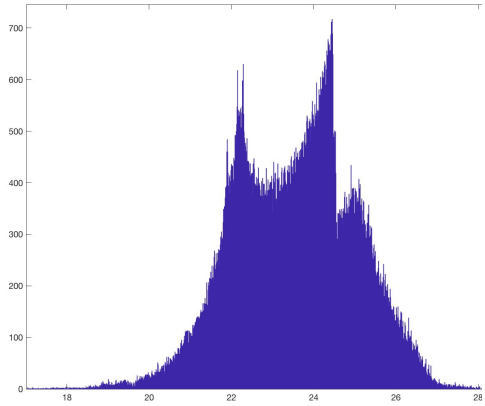

(c) using averaged time step T=200

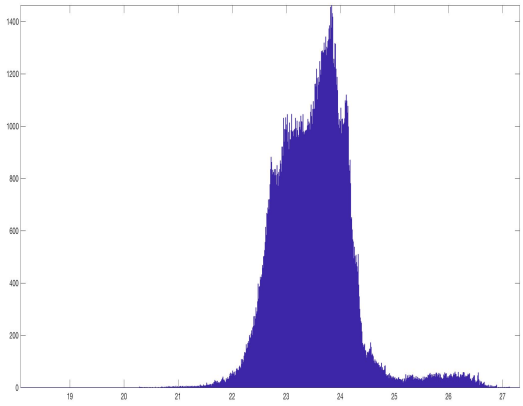

(d)using averaged time step T=500

Figure 3.3: histogram analysis of z solution in averaged Lorenz system which shows the portion of points that lies in different regions

$$X(K) = \sum_{n=0}^{N-1} x(n) e^{-2\pi kn/N}$$

$$x(n) = \frac{1}{N} \sum_{K=0}^{N-1} X(K) e^{2\pi kn/N}$$

where N is the total number of sequence. Following these rules, we get the spectra analysis in z solution which is shown in figure 3.4(a) to 3.4(d). The analysis in z is simplier and nicer compare to the analysis of x and y. All four figures have a dominant frequency in z-solution which is around 1.4Hz, whereas the amplitude or the height of the bump is decreasing. This corresponds with our previous observation that the Lorenz Attractor shrinks with increasing time step and eventually will be constrained in a small region. Figure 3.4(e) and 3.4(f) shows the spectral of x(t) and y(t) of original system and averaged system respectively. Those two figures illustrate that the spectra of x and y mostly locate at low frequency, with lots of noises in high frequency. This prove the existence of chaos in x and y, and a lack of dominant frequency. Alvarez and his collaborators made same observation that there exists a spectrum peak in z solution which reflects a nearly-invariant short-time period. And there exists an inherent frequency in Lorenz attractor which is uniquely determined by the value of parameters.

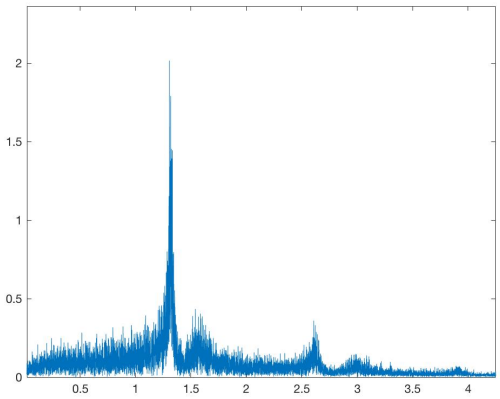

(a) spectral analysis of original z-solution

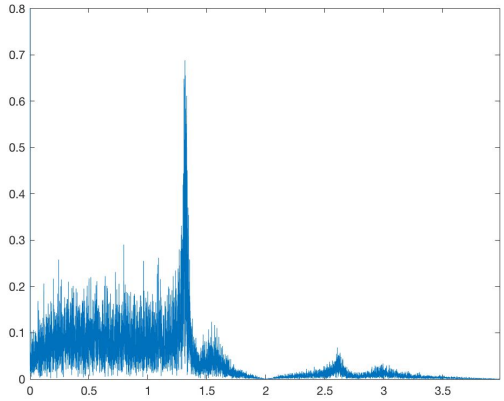

(b) using averaged time step T=50

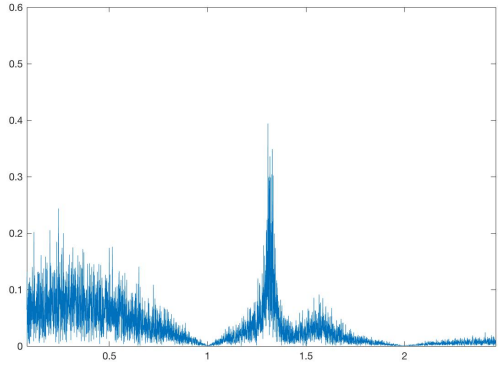

(c) using averaged time step T=100

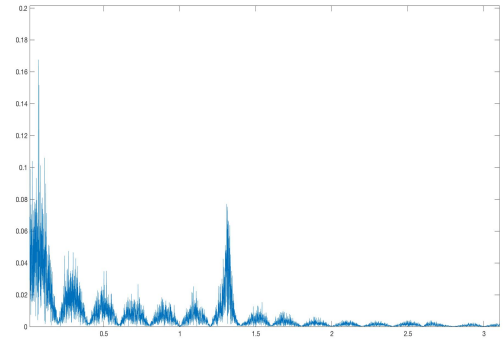

(d) using averaged time step T=500

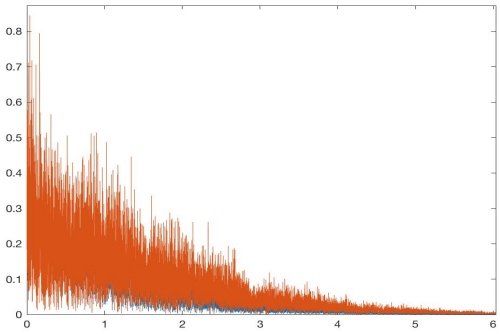

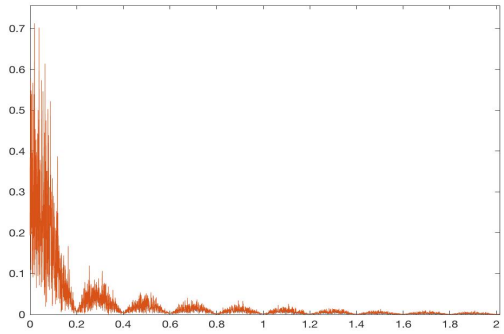

(e) spectral analysis of original x, y solution (f) analysis of averaged x, y solution using time step 500

Figure 3.4: spectra analysis of averaged z solution using different time step

3.4 Error Analysis and Prediction Analysis

As previously mentioned, Lorenz found the chaotic behaviors accidentally because of the rounding error. In fact, there is always uncertainty when computing the chaotic model. Hence, it is unrealistic to predict the long-term future. However, the average system gives a practicable model with higher predictability. The algorithm of Parlitz (1998) is used to estimate the unpredictability of the sliding averaged Lorenz system for different averaging time steps (Dwivedi, 2007). For two nearby initial conditions $x_0 + \delta_0$ and x_0, the initial error is $e_0 = ||\delta_0||$. At time k, the error $e_k = ||\delta_k||$ clearly depends on x_0, e_0. An appropriate measure of the unpredictability of x_0 at time $t = k$ is $u(x_0, k) = \log_2(e_k/e_0)$. A general measure of unpredictability, $u(k)$, is calculated by averaging $u(x_0, k)$ over different initial conditions. A smaller attractor implies a smaller expectated value of e_k and therefore a smaller $u(k)$, with a greater predictability.

The results are summarized in figure 3.5. From the figure, it is clear that the averaged system has greater predictability with increasing time step m. Hence, increasing the averaging time step leads to a greater predictability due to a smaller attractor.

Meanwhile, Dwidedi, Mittal and Pandey uses NLPCA technique of Hsieh (2004) and the resulted FEV statistic from NLPCA to measure the predictability. The FEV statistic from NLPCA as a measure of predictability is different from the predictability measures based on error growth rate. The latter assume that the unpredictability happens due to errors in the initial conditions. "The former measures the extent to which it is possible to model the observed time series by a deterministic system." (Dwivedi, 2007) In short, the measure of predictability reveals identical conclusion. As the length of sliding average increases, the prediction error decreases and therefore predictability increases.

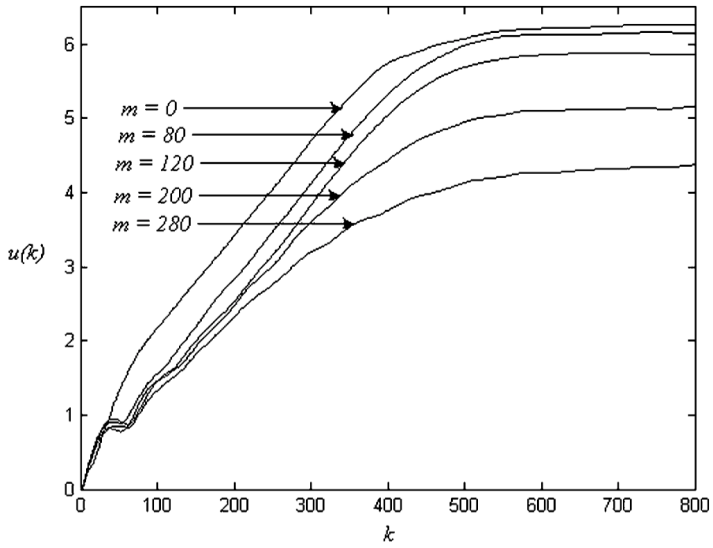

Figure 3.5: Plot of the unpredictability measure u(k) versus the prediction time steps, k, for different moving average steps,m [figure was drawn by Suneet Dwivedi, Ashok Kumar Mittal, and Avinash Chandra Pandey]

Chapter 4

Cusp Map Analysis

The cusp map is a useful tool to analyze the behavior of Lorenz map. It is calculated by first evolving the model for an arbitrary initial condition for a long enough time, and then notes down the successive local max value of z. This map reduces the three dimensional model to a one dimensional map. There indeed exists inevitable loss of information. However, most interesting properties are reserved. The map has the form of a cusp. And from the map, it is possible to predict the next maximum value of z, $z_{max}(n+1)$, from the current maximum value of z which is $z_{max}(n)$. Li and Zhang (2013) point out that even though the Lorenz system is nonlinear and unpredictable, the alternation between two branches is regular and predictable. Their work mainly focus on the double-cusp map, which is generated from the forced Lorenz system, and proves that the movement of z_{max} plays an important role. In the original Lorenz system that uses typical parameters without forcing, the model transfers to the other state when z_{max} crosses an critical value.

The cusp map for Lorenz system is given in figure 4.1. It depicts the cusp map for original Lorenz system using typical parameter and initial condition $(2, 5, 1)$. The light blue line is the line $z_{max}(n) = z_{max}(n+1)$. First, the peaks of two branches of the cusp

map overlap each other, reflecting that the critical value for alternation from positive branch to negative branch and from negative branch to positive branch of Lorenz system are the same. Starting from the first max value of z, z_{max} jumps between these two branches and getting closer to the peak. If the model runs for a long enough time, the z_{max} will be stable at the peak as well as the critical value of alternation. The maximum value of z is around 48 and the valid interval is from 28 to 48. The cusp map also implies a slow convergence of attractors since it intersects with the line $z_{max}(n) = z_{max}(n+1)$ at one point. This behavior means that an arbitrary trajectory will wander around the attractor for a very long time before it eventually collapse to the attractor. And each time the orbit gets close to the attractor, it will take a long time getting out of the region.

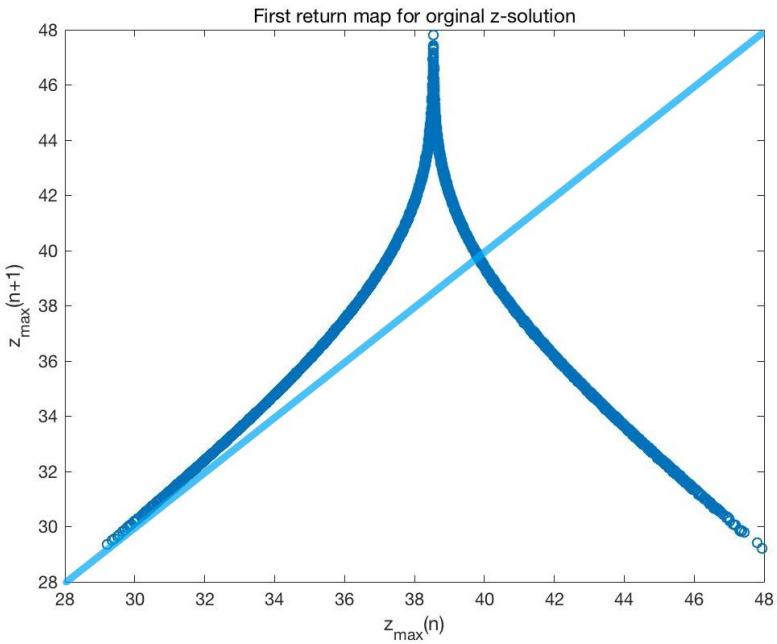

Figure 4.1: Cusp map of original Lorenz model (dark blue line) which intersects with the line $z_{max}(n) = z_{max}(n+1)$ (light blue line)

Chapter 5

Results and Interpretation

In chapter 3, we discuss the dynamics of averaged Lorenz System from several different perspectives. And chapter 4 uses cusp map to demonstrate the transition time between two regions of Lorenz attractors is predictable. In this chapter I will conclude those observations. In general, the averaged Lorenz Attractor remains some nice properties as the orignal Lorenz system. Furthermore, it maintains other nice qualities that the original system doesn't have and those qualities have a great contribution in long term climate prediction.

One of the significant conclusions is that the averaged Lorenz system does have periodicity in z-solution. Even with noises, this dominant periodicity implies that we can at least predict the movement of z(t) to some extent. The periodic climate event is not exact periodic and it fluctuates over a period. For example, the Pacific Decadal Oscillation (PDO) occurs in cycles of 25-45 years (Mantua et al., 1997), and the Atlantic Multi-decadal Oscillation (AMO), occurs on approximately 65-85 year cycles (Deser et al., 2010). Combining with the higher predictability that the averaged system has, the periodicity can be applied to explain some natural phenomenons.

The averaged system no longer depends on initial condition. Evolving different initial conditions over a long time gives rise to similar averaged Lorenz maps. With an increasing sliding average, we see that the attractors split into more parts that occupy smaller region in the phase space. And the shape of the attractors change from double-scroll to some small wandering circles. Eventually, the attractors will shrink to a stable small region that mostly lie between z=23.2 and z=24.5. Dwivedi, Mittal, and Chan (2007) showed that as the length of averaging time step increases, there is a decrease in the unpredictability, as well as the largest Lyapunov exponent. Since the Lyapunov exponent measures the predictability of a system and larger exponent implies lower predictability, the moving time-averaged Lorenz model does obtain greater predictability.

The cusp map further shows that the even though the future state is hard to predict, the transition time is predictable and we can narrow the prediction of future state in a small zone. Since the corresponding z_{max} always lie in nearby areas, this behavior reflects a higher predictability instead of predicting the exact state. Recall ENSO which does not show predictability in its long-term average, its cusp map however gives more information about the pattern of the event and this will be proved in later chapters.

Chapter 6

Application to Climate

6.1 El Nino

Lorenz System is a nonlinear model with climate background. Due to its symmetric structures around two strange attractors, some mathematicians believe that the two peaks of the model reflect the two opposite characteristics of climate system, as drought and flood, high and low temperature, strong and weak of monsoon. In fact, many climate phenomenons have this double-cusp properties. Sikka and Gdgil found that the intertropical convergence zone (ITCZ) related to large scale monsoon precipitation has double-cusp structure. Christiansen also found climate change with double-cusp properties in stratospheric atmosphere. These observations prove the feasibility of Lorenz System on basic properties of climate phenomenon.

But in general, it is unrealistic to give an exact physical meaning of Lorenz System since it is so simple whereas the actual climate depends on more factors. But it gives a qualitative behavior of atmosphere. I will analyze the most typical chaotic natural movement, El Nino and Southern Oscillation (ENSO), to verify the feasibility of

the averaged Lorenz model. ENSO is a coupled ocean-atmosphere system[9]. It involves fluctuating ocean temperatures in the central and eastern equatorial Pacific with changes in the atmosphere[9]. It will directly result a periodic variation in sea surface temperature (SST). ENSO is a periodic event that occurs every 6-8 years and usually last for at least three months. It happens around October and last to March next year. The most typical phenomenon that represent ENSO event is SST. El Nino leads to an extremely warm SST above average and La Nina results colder SST than usual.

Oceanic Nino Index (ONI) is a standard component that NOAA uses for identifying El Nino. It tracks running 3-month average SST in the east-central tropical Pacific between 120°-170°W (Niño 3.4 region). If ONI is above 0.5, then El Nino conditions start. If on the contrary, ONI is below -0.5, then La Nino conditions, which are the opposite of El Nino, start. National weather service gives all the ONI index about ENSO that happens from 1950 to 2019 and I will use these index to show that the method of taking sliding average is feasible for chaotic system.

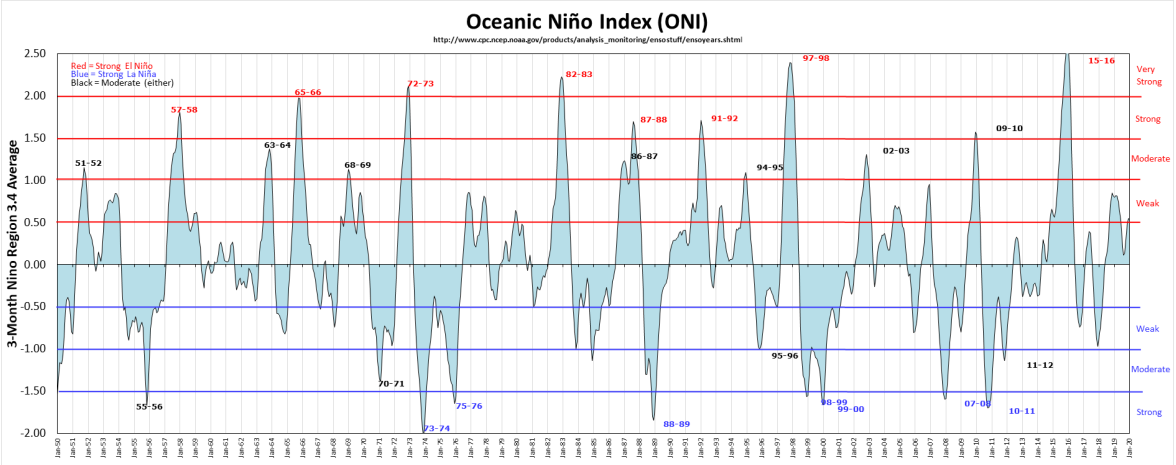

Figure 6.1: ONI of ENSO from 1950 to 2019 (data collected from National Weather Service, graphed by Golden Gate Weather Services)

Figure 6.1 plots the first ONI which is the SST average from December to January on next year. From the figure, El Nino and La Nina occurs consecutively year by year. From the original data provided by National Weather Service, the occurrence of El Nino usually corresponds to the first three ONI terms greater than 0.5 which ran through December to next April. Similarly, the occurrence of La Nina showed an lower than -0.5 ONI for the first three averages, indicating the region is much cooler than usual. El Nino and La Nina happens alternately resulting in unusual SST. Both events have significant influence on other areas on precipitation, climate, wind and etc. If we only consider the intensity of ONI, then a strong ONI indicates either El Nino or La Nina condition occurs. Hence, the absolute value of ONI is used to verify if the intensity of current event has any impact in future events. The mean of ONI is not used since it does not differ a lot from the original ONI and correlation is inevitable. From the original data, the first three ONI terms are usually similar to each other, indicating the continuation of the event. And by using the absolute value of ONI instead of its mean, it is more straightforward to analyze the correlation between events. Both El Nino and La Nino carry out a sum usually greater than 4 and normal year has a sum around 1. Figure 6.2 depicts the dynamics of the cusp map of ENSO by finding its local max or min using only intensity. It finds the relation between current extrema and next extrema using January's ONI, which implies the relation between the current event and the next possible event.

From Fig 6.2, the points accumulate at three parts: upper left, upper right and lower right. The x-axis for upper left region is constrained in [-2,-1] and y-axis is constrained in [0.5,2]. The horizontal restriction [-2,-1] correspond to the occurrence of La Nina, which is below -0.5. The vertical restriction [0.5,2] illustrates the occurrence of El Nino. So the upper left region shows the occurrence of current La Nina indicates the next possible event will be El Nino. The the current event of El Nino correspond to the lower right region where the horizontal restriction is [1,2.5], and the next possible events

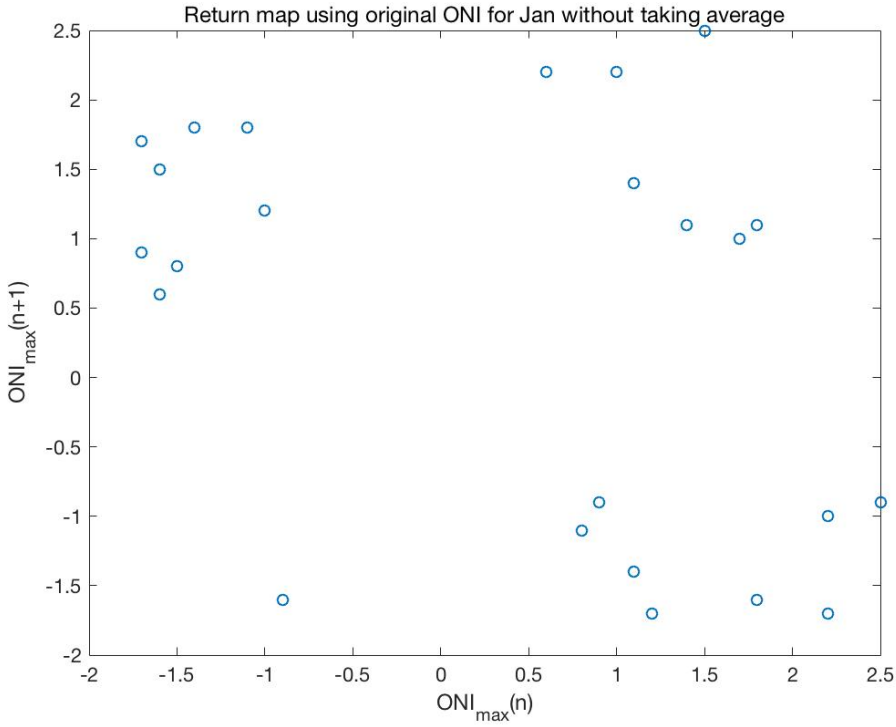

Figure 6.2: Return map of ENSO from 1950 to 2019

lie in [-1,-2] which are La Nina. So the upper left and lower right region demonstrate the alternate occurrence of El Nino and La Nina. The upper right region, which lies in [0.5,2] and [1,2.5], implies that under some circumstances, the current El Nina implies the next possible event will still be El Nina instead of La Nino. This plot represents the nature of ENSO and can be used to predict what the next event is. If the current event is La Nino, then it is almost certain that the next event will be El Nino. However, it is not obvious that there is any pattern in Fig 6.2 or if it has a dominant period even though ENSO typically occurs every 6 to 8 years. Indeed, the cusp map for Lorenz system shows the future trajectory jumps between two attractors. The corresponding return map for ENSO demonstrates that the ENSO event will jump between two strong events, El Nino and La Nina, which requires completely opposite conditions to occur.

6.2 Global Temperature

Global temperature represents the mean temperature over the entire surface of earth. Different from local temperature which depend heavily on cyclical events and unpredictable events such as local wind and precipitation, global temperature mainly depends on how much energy it receives from the sun. Thus, a one-degree change in global temperature requires a huge amount of energy from the sun. It is well known that the world is getting warmer. Figure 6.3 plots the change in global temperature from 1880 to 2020 with respect to the 1910 to 2000 average. The global temperature of a year is calculated using the year average.

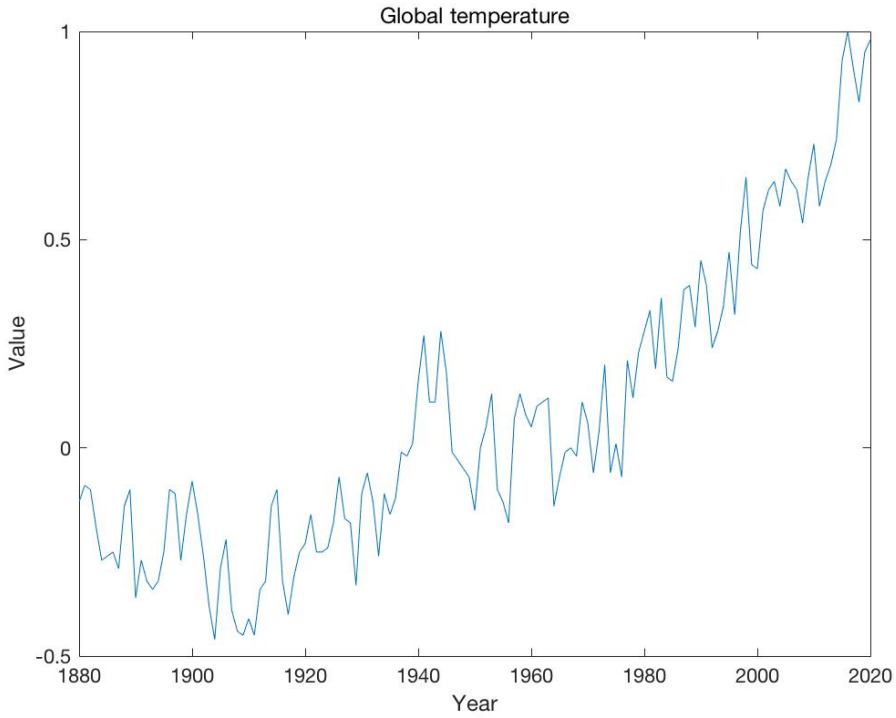

Figure 6.3: Change in Global Temperature from 1880 to 2020 (data collected from NOAA National Centers for Environmental information)

From the figure, it is apparent that even though the global temperature is increasing

from 1880, it begins drastically increasing since 1980 and reaches one-degree increase.

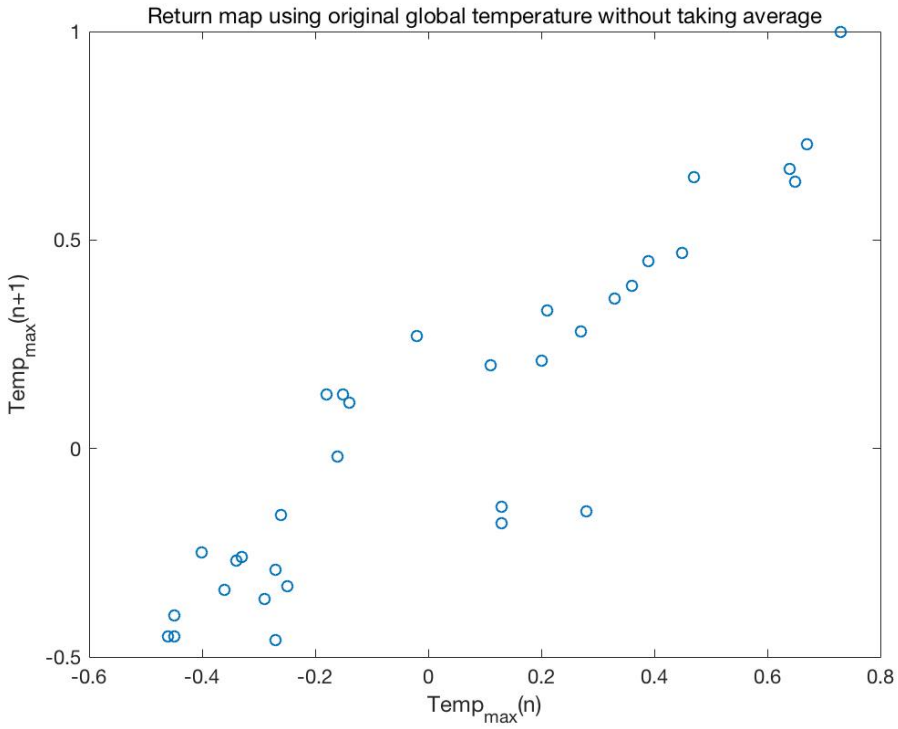

Figure 6.4: Return map for global temperature

Figure 6.4 plots the return map for global temperature from 1880 to 2020. It first finds the local maximum of global temperature and plot the relation between the current local max and the next local max which follow the same algorithm for plotting the return map for Lorenz system and ENSO. From Fig 6.4, it is more obvious that in the top right of the figure, there is a linear relation and global temperature steadily increases. The temperature above 0 in the upper right correspond to 1960 decade. So the global temperature after 1960 steadily increases. However, only a few points exist in the upper right corner, and point $(0.74, 1)$ demonstrating a drastic raise in global temperature. Return map shows the internal nature of a system. Using this linear relation, it is possible to predict the amount of time required to reach the two-degree change.

Figure 6.5 further compares the Global Temperature with its return map and its 30-year average. From 6.5(a), taking a long time average clearly shows the long-term trend of the climate which is gradually increasing. However, it neglects some important features such as the extreme cold year around 1910 and the extreme warm period around 1940. So in general, taking the average indeed can give us some information about a climate system. Nevertheless, that is not comprehensive. And the cusp map is a supplement. From figure 6.5(b), we can see that the cusp map also shows an increasing trend. Though the increasing trend is not as clear as shown by the 30-year average, the cusp map captures some important features of the system that 30-year average can not show, such as the cold period around 1910. Moreover, it catches the recent warmest year 2020 which 30-year average can not even cover. Therefore, the average and the return map together can better predict the future state of a system.

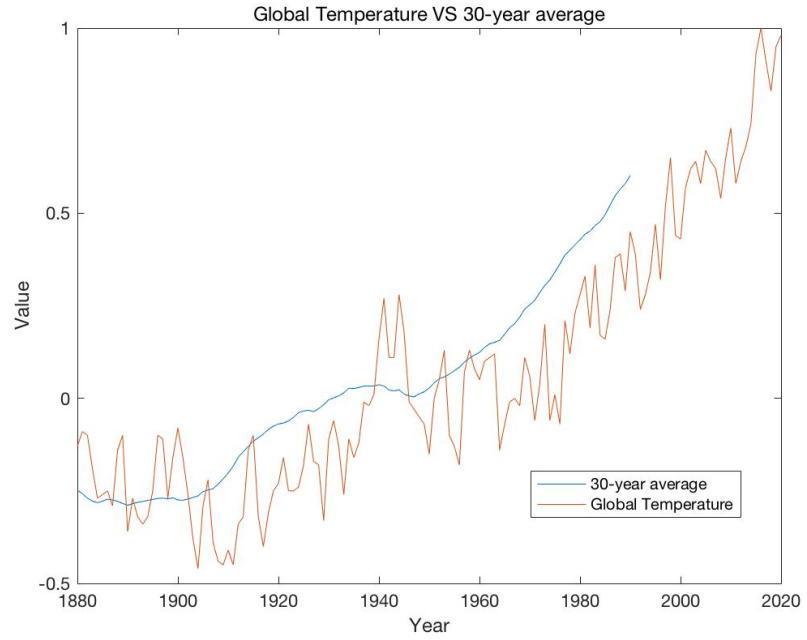

(a) compare Global Temperature with its 30-year average

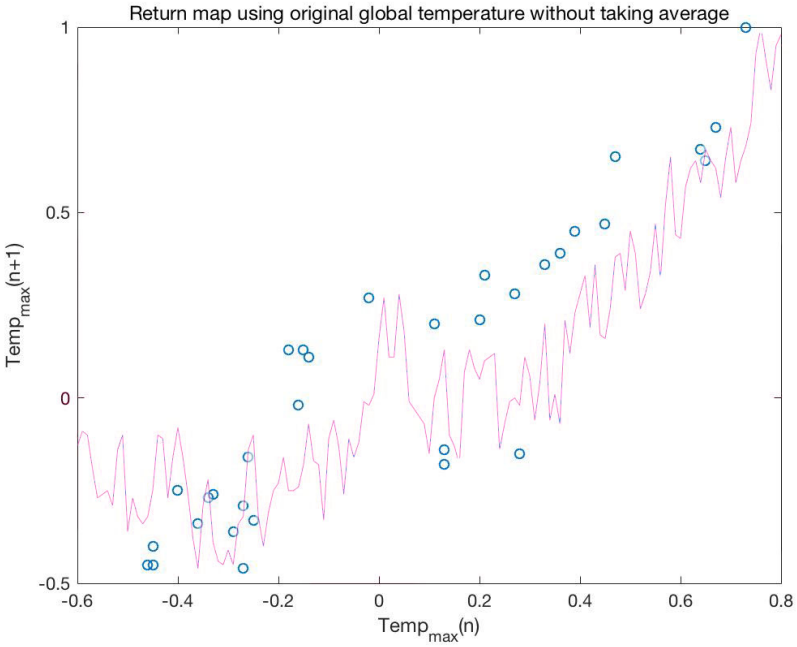

(b) compare Global Temperature with its return map (the purple line represent Global Temperature)

Figure 6.5: Compare Global Temperature with its return map and the 30-year average

Chapter 7

Future Work

There are several questions left. One question is what the averaging time should be in order to have a predictability and whether there exists a limit for averaging time step. If we take the averaging time step too small, then the averaged system behaves no difference from the original one. But if we take the averaging time step too large, then the averaged system should have no physical meaning. Hence, to what extent should the time step be is a question.

Another question is if the averaged Lorenz attractors can split infinitely. We have seen that the averaged Lorenz attractors can be divided into smaller regions as time step increases. And the converging zone of Lorenz attractors keeps shrinking. One may ask if the converging zone is possible to shrink to a line in the long run. However, it is still unclear if this process can keep running for infinite times.

Another intriguing field is the forcing Lorenz system which simply means the Lorenz system with forcing, either constant forcing or periodic forcing. Many climate factors, such as atmosphere and ocean temperature, can be modeled as forcing terms. And hence, the forced Lorenz system should have more practical meaning. In fact, Dwivedi,

Mittal, and Chan already proved that the averaged Lorenz system with forcing have even higher predictability. But more detailed analysis on its dynamics still deserves exploration.

References

[1] Douglas F. Elliott. *Handbook of Digital Signal Processing.* Elsevier, 1987.

[2] Jan Philipp Dietrich. "Phase Space Reconstruction using the frequency domain." 2008.

[3] S. H Strogatz. *Nonlinear Dynamics and Chaos.* Westview Press, 1994.

[4] Edward Lorenz. *The Essence of Chaos.* University of Washington Press, Seattle, 1993.

[5] J. Gleick. *Chaos: Making a New Science.* Viking, New York, 1987.

[6] Ai Bing Li and Li Feng Zhang. "Rules for predicting regime change in the Lorenz chaotic system based on the Lorenz map." *Physics Science*, 62(12), 2013.

[7] James Hateley. "The Lorenz system." *Lecture Notes.*

[8] Tiberiu Harko, Chor Yin Ho, Chun Sing Leung, and Stan Yip. "Jacobi stability analysis of the Lorenz system." *International Journal of Geometric Methods in Modern Physics*, 12(07), 2015.

[9] Mehta Mitaxi and Mittal A.K. "The Double-Cusp Map for the forced lorenz system." *International Journal of Geometric Methods in Modern Physics*, 12(07), 2015.

[10] Cvitanović Predrag, Artuso Roberto, Mainieri Ronnie, Tanner Gregor, and Vattay Gabor. *Chaos: Classical and Quantum.* Niels Bohr Institute, Copenhagen, 2012.

[11] Pradip K Pal and Shivani Shah. "Feasibility study of extended range atmospheric prediction through time average Lorenz attractor." *Indian Journal of Radio Space Physics*, 28:271–276, 1999.

[12] Karl Sigmund. "Time averages for unpredictable orbits of deterministic systems." *Annals of Operations Research*, 37(1):217–228, 1992.

[13] Suneet Dwivedi, Ashok Kumar Mittal, and Avinash Chandra Pandey. "Effect of averaging timescale on a forced Lorenz model." *Atmosphere-ocean*, 45(2):71–79, 2007.

[14] Olusegun SA Oluwole. "Deterministic Chaos, El Nino southern oscillation, and seasonal influenza epidemics." *Frontiers in Environmental Science*, 5:8, 2017.

[15] G. Alvarez, Shujun Li, Jinhu Liu, and Guanrong Chen. "Inherent frequency and spatial decomposition of the Lorenz chaotic attractor." *ArXiv e-prints*, 0406031.

[16] Alan Wolf, Jack B Swift, Harry L Swinney, and John A Vastano. "Determining Lyapunov exponents from a time series." *Physica D: Nonlinear Phenomena*, 16(3):285–317, 1985.

[17] Qiaobin Teng, Adam H Monahan, and John C Fyfe. "Effects of time averaging on climate regimes." *Geophysical research letters*, 31(22), 2004.

[18] Davide Faranda, Gabriele Messori, and Stéphane Vannitsem. "Attractor dimension of time-averaged climate observables: insights from a low-order ocean-atmosphere model." *Tellus A: Dynamic Meteorology and Oceanography*, 71(1):1–11, 2019.

[19] AM Selvam. "Nonlinear dynamics and chaos: Applications in atmospheric sciences." *Journal of Advanced Mathematics and Applications*, 1(2):181–205, 2012.

[20] FK Diakonos and P Schmelcher. "A turning point analysis of the ergodic dynamics of iterative maps." *International Journal of Bifurcation and Chaos*, 7(11):2459–2474, 1997.

[21] Edward N Lorenz. "Deterministic nonperiodic flow." *Journal of the atmospheric sciences*, 20(2):130–141, 1963.

[22] L Mark Berliner. "Statistics, probability and chaos." *Statistical Science*, pages 69–90, 1992.

[23] Burrus C.Sidney, Frigo Matteo, G.Johnson Steven, Pueschel Markus, and Selesnick Ivan. *Fast Fourier Transforms*. Rice University, Houston, Texas, 2012.

[24] Paul Heckbert. "Fourier transforms and the fast Fourier transform (FFT) algorithm." *Computer Graphics*, 2:15–463, 1995.

[25] Wanjun Huang and Duncan L MacFarlane. "Fast fourier transform and matlab implementation." *The University of Texas at Dallas. Dr. Duncan L. MacFarlane. Web*, 24, 2016.

[26] Sandy Black, David Christie, and Neil Finlayson. "Spectral analysis of nonlinear systems." *Theoretical and Applied Mechanics*, 37(2):111–137, 2010.

[27] Brian R Hunt, Judy A Kennedy, Tien-Yien Li, and Helena E Nusse. *The theory of chaotic attractors*. Springer Science & Business Media, 2013.

[28] William Arnold Barnett. *Dynamic Disequilibrium Modeling: Theory and Applications: Proceedings of the Ninth International Symposium in Economic Theory and Econometrics*, volume 9. Cambridge University Press, 1996.